

Polymersomes with Ionic Liquid Interiors Dispersed in Water

Zhifeng Bai[†] and Timothy P. Lodge^{*,†,‡}

*Department of Chemistry and Department of Chemical Engineering & Materials Science,
University of Minnesota, Minneapolis, Minnesota 55455, United States*

Received August 27, 2010; E-mail: lodge@umn.edu

Abstract: We describe polymersomes with ionic liquid interiors dispersed in water. The vesicles are prepared via a simple and spontaneous migration of poly(butadiene-*b*-ethylene oxide) (PB-PEO) block copolymer vesicles from a hydrophobic ionic liquid, 1-ethyl-3-methylimidazolium bis(trifluoromethylsulfonyl)imide ([EMIM][TFSI]), to water at room temperature. As PB is insoluble in both water and [EMIM][TFSI] and PEO is well solvated in both media, the vesicles feature a PB membrane with PEO brushes forming both interior and exterior coronas. The robust and stable PB-PEO vesicles migrate across the liquid–liquid interface with their ionic liquid interiors intact and form a stabilized aqueous dispersion of vesicles enclosing microscopic ionic liquid pools. The nanostructure of the vesicles with ionic liquid interiors dispersed in water is characterized by direct visualization using cryogenic transmission electron microscopy. Upon heating, the vesicles can be quantitatively transferred back to [EMIM][TFSI], thus enabling facile recovery. The reversible transport capability of the shuttle system is demonstrated by the use of distinct hydrophobic dyes, which are selectively and simultaneously loaded in the vesicle membrane and interior. Furthermore, the fluorescence of the loaded dyes in the vesicles enables probing of the microenvironment of the vesicular ionic liquid interior through solvatochromism and direct imaging of the vesicles using laser scanning confocal microscopy. This vesicle system is of particular interest as a nanocarrier or nanoreactor for reactions, catalysis, and separations using ionic liquids.

Introduction

Polymer vesicles,¹ also known as polymersomes, are microscopic containers with internal fluid pools enclosed by a thin membrane self-assembled from amphiphilic block copolymers. Compared to liposomes, their natural analogue, polymer vesicles possess significantly thicker membranes, leading to remarkable enhancement in their robustness and stability.² Moreover, polymersome properties can be widely tailored via the attributes of the block copolymer, for example, in terms of dimension,^{3,4} structure,^{5–9} and chemical functionality.^{10–12} Polymersomes have received considerable attention for potential applications in nanoreactors,^{13–15} material fabrication templates,¹⁶ drug

delivery,^{17,18} and others.^{19–23} The vesicle interior, where encapsulation or reactions typically occur, is of particular importance. Polymersomes are commonly dispersed in water and thus have aqueous interiors. Although the dispersion of vesicles in other fluids may allow for broader applications, examples are rather limited, e.g., in organic solvents,^{24–27} ionic liquids,²⁸ and supercritical carbon dioxide.²⁹

Here, distinct from canonical vesicles with the same fluid inside and outside, we report polymer vesicles with hydrophobic

[†] Department of Chemistry.

[‡] Department of Chemical Engineering and Materials Science.

- (1) Discher, D. E.; Eisenberg, A. *Science* **2002**, *297*, 967–973.
- (2) Discher, B. M.; Won, Y. Y.; Ege, D. S.; Lee, J. C. M.; Bates, F. S.; Discher, D. E.; Hammer, D. A. *Science* **1999**, *284*, 1143–1146.
- (3) Bermudez, H.; Brannan, A. K.; Hammer, D. A.; Bates, F. S.; Discher, D. E. *Macromolecules* **2002**, *35*, 8203–8208.
- (4) Wang, W.; McConaghy, A. M.; Tetley, L.; Uchegbu, I. F. *Langmuir* **2001**, *17*, 631–636.
- (5) Zhang, L. F.; Eisenberg, A. *Science* **1995**, *268*, 1728–1731.
- (6) van Hest, J. C. M.; Delnoye, D. A. P.; Baars, M. W. P. L.; van Genderen, M. H. P.; Meijer, E. W. *Science* **1995**, *268*, 1592–1595.
- (7) Yu, G. R.; Eisenberg, A. *Macromolecules* **1998**, *31*, 5546–5549.
- (8) Li, Z.; Hillmyer, M. A.; Lodge, T. P. *Nano Lett.* **2006**, *6*, 1245–1249.
- (9) Percec, V.; et al. *Science* **2010**, *328*, 1009–1014.
- (10) Antonietti, M.; Forster, S. *Adv. Mater.* **2003**, *15*, 1323–1333.
- (11) Blanazs, A.; Armes, S. P.; Ryan, A. J. *Macromol. Rapid Commun.* **2009**, *30*, 267–277.
- (12) Hawker, C. J.; Wooley, K. L. *Science* **2005**, *309*, 1200–1205.
- (13) Vriezema, D. M.; Aragonés, M. C.; Elemans, J. A. A. W.; Cornelissen, J. J. L. M.; Rowan, A. E.; Nolte, R. J. M. *Chem. Rev.* **2005**, *105*, 1445–1489.

- (14) Kita-Tokarczyk, K.; Grumelard, J.; Haefele, T.; Meier, W. *Polymer* **2005**, *46*, 3540–3563.
- (15) Kim, K. T.; Meeuwissen, S. A.; Nolte, R. J. M.; van Hest, J. C. M. *Nanoscale* **2010**, *2*, 844–858.
- (16) Hamley, I. W. *Angew. Chem., Int. Ed.* **2003**, *42*, 1692–1712.
- (17) Discher, D. E.; Ahmed, F. *Annu. Rev. Biomed. Eng.* **2006**, *8*, 323–341.
- (18) Meng, F.; Zhong, Z.; Feijen, J. *Biomacromolecules* **2009**, *10*, 197–209.
- (19) Graff, A.; Sauer, M.; Van Gelder, P.; Meier, W. *Proc. Natl. Acad. Sci. U.S.A.* **2002**, *99*, 5064–5068.
- (20) Lin, J.; Silas, J. A.; Bermudez, H.; Milam, V. T.; Bates, F. S.; Hammer, D. A. *Langmuir* **2004**, *20*, 5493–5500.
- (21) Ghoroghchian, P. P.; Frail, P. R.; Susumu, K.; Blessington, D.; Brannan, A. K.; Bates, F. S.; Chance, B.; Hammer, D. A.; Therien, M. J. *Proc. Natl. Acad. Sci. U.S.A.* **2005**, *102*, 2922–2927.
- (22) Boerakker, M. J.; Botterhuis, N. E.; Bomans, P. H. H.; Frederik, P. M.; Meijer, E. M.; Nolte, R. J. M.; Sommerdijk, N. *Chem.—Eur. J.* **2006**, *12*, 6071–6080.
- (23) Krack, M.; Hohenberg, H.; Kornowski, A.; Lindner, P.; Weller, H.; Forster, S. *J. Am. Chem. Soc.* **2008**, *130*, 7315–7320.
- (24) Soo, P. L.; Eisenberg, A. *J. Polym. Sci., Part B* **2004**, *42*, 923–938.
- (25) Bang, J.; Jain, S.; Li, Z.; Lodge, T. P.; Pedersen, J. S.; Kesselman, E.; Talmon, Y. *Macromolecules* **2006**, *39*, 1199–1208.
- (26) Njikang, G.; Han, D.; Wang, J.; Liu, G. *Macromolecules* **2008**, *41*, 9727–9735.

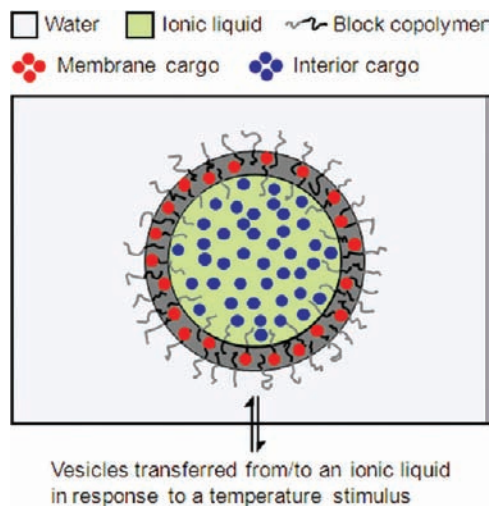


Figure 1. Schematic illustration of vesicles with ionic liquid interiors dispersed in water, and their use in reversible transport of two kinds of cargoes simultaneously and selectively loaded in the membrane and interior, to and out of water by a vesicle shuttle.

ionic liquid interiors dispersed in water (Figure 1). The robust membrane provides a stable enclosure for the internal ionic liquid pool, while the corona enables dispersion of the microscopically heterogeneous system. To our knowledge, this is the first example of vesicles in water whereby another fluid is located in the interior. This structure therefore represents a new kind of microemulsion, in which one immiscible fluid is compartmentalized within a matrix of another and stabilized not by a surfactant monolayer^{30,31} but by a bilayer. This architecture is reminiscent of cells, in which the cytosol might have quite different reagent concentrations than the exterior, but is also quite distinct in that essentially no mixing of interior and exterior fluids should occur. The enclosed ionic liquid belongs to a class of solvents well recognized as promising media for reactions^{32–34} and separations³⁵ due to their negligible volatility, widely tunable solvation properties, and remarkable chemical and thermal stability.³⁶ Furthermore, the corona blocks endow the vesicles with thermal responsiveness to migrate reversibly between an aqueous phase and an ionic liquid phase. Stimuli-responsive vesicles are currently under active study using polymers sensitive to various stimuli^{37,38} such as temperature,^{39–42} pH,^{43–46} and light.⁴⁷ In most cases the stimulus is used to exert control over membrane stability and

permeability. Responsive vesicles that migrate across a liquid–liquid interface are rare,⁴⁸ however, they are clearly of interest for controlled delivery and recovery of, e.g., therapeutic agents or catalysts. Recently, Deming and co-workers developed robust poly(arginine-*b*-leucine) block copolypeptide vesicles in water that were able to migrate to chloroform and back again with large molecules carried in their interiors, through binding the polyarginine corona with suitable hydro/lipophilic counterions.⁴⁸ Such an approach is an elegant example that mimics membrane transport.

One motivation for the current work arises from the recently reported micelle shuttle—a reversible, quantitative, and intact transfer of poly((1,2-butadiene)-*b*-ethylene oxide (PB-PEO) block copolymer micelles between water at room temperature and a hydrophobic ionic liquid at an elevated temperature.⁴⁹ As the PB block is insoluble in both water and the ionic liquid and as the PEO block is well dissolved in both phases, these micelles experience no tendency to restructure during the transfer between phases. The transfer is driven by the lower critical solution temperature (LCST) phase behavior, i.e., solubility decreases upon heating, of the PEO corona in water.⁵⁰ The generality of this phenomenon is suggested by successful demonstration using other block copolymers^{51–53} and different ionic liquids.⁵⁰ Since favorable thermal^{54–57} and light⁵⁸ responsiveness of certain polymers in ionic liquids have been observed and applied to the self-assembly of block copolymers,^{59–61} the shuttle system can be endowed with desired properties, such as controlled loading and release.⁵¹ The transfer thermodynamics and mechanism have also been studied in detail.⁶² Effective transport of various cargoes loaded in the micelle core in the biphasic system has also been demonstrated.^{52,62} This simple and tailorable shuttle should find applications in systems exploiting ionic liquids for reactions, catalysis, and separations.

- (27) Di Cola, E.; Lefebvre, C.; Deffieux, A.; Narayanan, T.; Borsali, R. *Soft Matter* **2009**, *5*, 1081–1090.
 (28) He, Y.; Li, Z.; Simone, P. M.; Lodge, T. P. *J. Am. Chem. Soc.* **2006**, *128*, 2745–2750.
 (29) Edmonds, W. F.; Hillmyer, M. A.; Lodge, T. P. *Macromolecules* **2007**, *40*, 4917–4923.
 (30) Eastoe, J.; Gold, S.; Rogers, S. E.; Paul, A.; Welton, T.; Heenan, R. K.; Grillo, I. *J. Am. Chem. Soc.* **2005**, *127*, 7302–7303.
 (31) Gao, Y.; Han, S.; Han, B.; Li, G.; Shen, D.; Li, Z.; Du, J.; Hou, W.; Zhang, G. *Langmuir* **2005**, *21*, 5681–5684.
 (32) Dupont, J.; de Souza, R. F.; Suarez, P. A. Z. *Chem. Rev.* **2002**, *102*, 3667–3692.
 (33) Parvulescu, V. I.; Hardacre, C. *Chem. Rev.* **2007**, *107*, 2615–2665.
 (34) van Rantwijk, F.; Sheldon, R. A. *Chem. Rev.* **2007**, *107*, 2757–2785.
 (35) Han, X.; Armstrong, D. W. *Acc. Chem. Res.* **2007**, *40*, 1079–1086.
 (36) Rogers, R. D.; Seddon, K. R. *Science* **2003**, *302*, 792–793.
 (37) Li, M. H.; Keller, P. *Soft Matter* **2009**, *5*, 927–937.
 (38) Du, J. Z.; O'Reilly, R. K. *Soft Matter* **2009**, *5*, 3544–3561.
 (39) Qin, S. H.; Geng, Y.; Discher, D. E.; Yang, S. *Adv. Mater.* **2006**, *18*, 2905–2909.
 (40) Abbas, S.; Li, Z.; Hassan, H.; Lodge, T. P. *Macromolecules* **2007**, *40*, 4048–4052.

- (41) Sundararaman, A.; Stephan, T.; Grubbs, R. B. *J. Am. Chem. Soc.* **2008**, *130*, 12264–12265.
 (42) Moughton, A. O.; O'Reilly, R. K. *Chem. Commun.* **2010**, *46*, 1091–1093.
 (43) Liu, F. T.; Eisenberg, A. *J. Am. Chem. Soc.* **2003**, *125*, 15059–15064.
 (44) Bellomo, E. G.; Wyrsta, M. D.; Pakstis, L.; Pochan, D. J.; Deming, T. J. *Nat. Mater.* **2004**, *3*, 244–248.
 (45) Du, J. Z.; Tang, Y. P.; Lewis, A. L.; Armes, S. P. *J. Am. Chem. Soc.* **2005**, *127*, 17982–17983.
 (46) Yu, S.; Azzam, T.; Rouiller, I.; Eisenberg, A. *J. Am. Chem. Soc.* **2009**, *131*, 10557–10566.
 (47) Mabrouk, E.; Cuvelier, D.; Brochard-Wyart, F.; Nassoy, P.; Li, M. H. *Proc. Natl. Acad. Sci. U.S.A.* **2009**, *106*, 7294–7298.
 (48) Holowka, E. P.; Sun, V. Z.; Kamei, D. T.; Deming, T. J. *Nat. Mater.* **2007**, *6*, 52–57.
 (49) He, Y.; Lodge, T. P. *J. Am. Chem. Soc.* **2006**, *128*, 12666–12667.
 (50) Bai, Z.; He, Y.; Lodge, T. P. *Langmuir* **2008**, *24*, 5284–5290.
 (51) Bai, Z.; He, Y.; Young, N. P.; Lodge, T. P. *Macromolecules* **2008**, *41*, 6615–6617.
 (52) Bai, Z.; Lodge, T. P. *Langmuir* **2010**, *26*, 8887–8892.
 (53) Guerrero-Sanchez, C.; Gohy, J. F.; D'Haese, C.; Thijs, H.; Hoogenboom, R.; Schubert, U. S. *Chem. Commun.* **2008**, 2753–2755.
 (54) Ueki, T.; Watanabe, M. *Chem. Lett.* **2006**, *35*, 964–965.
 (55) Ueki, T.; Watanabe, M. *Langmuir* **2007**, *23*, 988–990.
 (56) Tsuda, R.; Kodama, K.; Ueki, T.; Kokubo, H.; Imabayashi, S.; Watanabe, M. *Chem. Commun.* **2008**, 4939–4941.
 (57) Lee, H. N.; Lodge, T. P. *J. Phys. Chem. Lett.* **2010**, *1*, 1962–1966.
 (58) Ueki, T.; Yamaguchi, A.; Ito, N.; Kodama, K.; Sakamoto, J.; Ueno, K.; Kokubo, H.; Watanabe, M. *Langmuir* **2009**, *25*, 8845–8848.
 (59) He, Y.; Lodge, T. P. *Chem. Commun.* **2007**, 2732–2734.
 (60) Ueki, T.; Watanabe, M.; Lodge, T. P. *Macromolecules* **2009**, *42*, 1315–1320.
 (61) Tamura, S.; Ueki, T.; Ueno, K.; Kodama, K.; Watanabe, M. *Macromolecules* **2009**, *42*, 6239–6244.
 (62) Bai, Z.; Lodge, T. P. *J. Phys. Chem. B* **2009**, *113*, 14151–14157.

Shuttles of nanoparticles between water and organic solvents have shown similar promise.^{63–67}

However, whereas the previously reported micelle shuttles focused on spherical micelles, a vesicle shuttle can allow for different possible applications. One key difference between a vesicle and a spherical micelle as a transport vehicle is the particle volume and thus carrying capacity. A typical micellar core volume is 10^3 – 10^4 nm³, whereas that of a vesicle can easily exceed 10^6 – 10^7 nm³, enabling delivery of larger molecules such as proteins.⁶⁸ Furthermore, the interior of the vesicle is full of one solvent and may be carried to the other solvent upon the transfer. Thus, both solvophilic and solvophobic reagents may be transported concurrently in the vesicle interior and membrane, respectively, which may prove to be useful for synergistic applications such as cascade reactions.^{69,70} In fact, liquid–liquid biphasic systems involving ionic liquids have shown significant promise in biphasic organometallic^{32,33} and biocatalysis³⁴ and extraction.³⁵ A dispersion of microscopic ionic liquid pools in water (or vice versa) enabling rapid mixing, thermal uniformity, and easy separation is thus highly desirable. For example, for a reaction in the aqueous dispersion, a catalyst may be preserved in the ionic liquid pocket that is tailored for optimum performance and thereafter recovered simply via the vesicle migration. In short, this approach promises to marry the advantages of both homogeneous and heterogeneous catalysis.

To this end, we demonstrate PB-PEO block copolymer vesicles in water with interiors filled with the common hydrophobic ionic liquid, 1-ethyl-3-methylimidazolium bis(trifluoromethylsulfonyl)imide ([EMIM][TFSI]). The vesicles are prepared by a spontaneous vesicle transfer from [EMIM][TFSI] to water upon addition of water to a vesicle solution in [EMIM][TFSI]. The vesicle membrane is formed of PB blocks, whereas the interior and exterior coronas comprise PEO chains; this is the thermodynamically preferred configuration in water, in the ionic liquid, or with an ionic liquid interior and an aqueous exterior. The stable and robust PB-PEO vesicles migrate intact across the liquid–liquid interface and thereby transport their ionic liquid interiors to water, as evidenced by direct visualization of the resultant vesicles using cryogenic transmission electron microscopy (cryo-TEM). Cryo-TEM also provides detailed packing characterization of the vesicles. The vesicles can be easily and quantitatively recovered through a transfer back to the ionic liquid phase upon heating. The transport capability of the shuttle system is demonstrated by the reversible delivery of distinct hydrophobic dyes, which are selectively and simultaneously loaded in the vesicle membrane and interior, from [EMIM][TFSI] to water. Moreover, the loading of a solvatochromic fluorescence dye in the vesicle interior allows

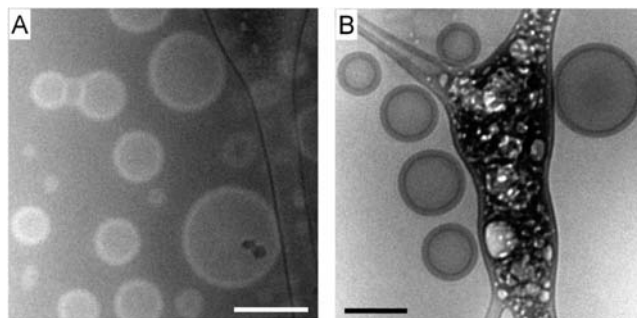


Figure 2. Cryo-TEM images of PB-PEO vesicles formed in [EMIM][TFSI] (A) and water (B). Scale bars, 200 nm.

for the probing of the interior microenvironment. The vesicles loaded with fluorescence dyes in the membrane and/or interior can also be characterized by imaging using laser scanning confocal microscopy (LSCM).

Results and Discussion

Vesicles were initially self-assembled from a PB-PEO block copolymer, with a 14 kDa PB block, a 4.5 kDa PEO block, and a polydispersity of 1.03,⁷¹ by dissolution of a thin film of the copolymer in [EMIM][TFSI]. The resulting cloudy dispersion reflects the formation of relatively large vesicles. The nanostructure of the vesicles was characterized by cryo-TEM. As shown in Figure 2A, due to the lower electron density (ρ_e) of the PB block compared to [EMIM][TFSI], the closely packed PB membrane is visualized as the light domains, while the well-solvated PEO corona is invisible against the dark [EMIM][TFSI] matrix. This particular PB-PEO block copolymer also forms vesicles in water (Figure 2B), in agreement with previous results;⁷¹ here the PB membrane forms the darker domains, due to its higher ρ_e than the aqueous matrix. The similarity of the phase behavior of PB-PEO block copolymers in water⁷² and in [EMIM][TFSI]⁷³ has also been documented, indicating comparable selectivity of the two solvents toward the diblocks. Some coexisting spherical and worm-like micelles are also observed in [EMIM][TFSI]. This polymorphism is not uncommon for PB-PEO block copolymers in water^{72,74} and ionic liquids²⁸ and for other strongly amphiphilic systems,⁷⁵ due to the kinetically trapped structures with extremely low critical aggregation concentrations and negligible chain exchange. For example, the negligible solubility of the PB block in both water⁷⁴ and [EMIM][TFSI]⁷⁶ has been confirmed by neutron scattering measurements, which show no chain exchange between PB-PEO micelles over a time scale of days. If desired, vesicles with well-controlled morphology and size can be achieved using specific preparation strategies.^{77–80}

(63) Chechik, V.; Zhao, M.; Crooks, R. M. *J. Am. Chem. Soc.* **1999**, *121*, 4910–4911.

(64) Marcilla, R.; Curri, M. L.; Cozzoli, P. D.; Martinez, M. T.; Loinaz, I.; Grande, H.; Pomposo, J. A.; Mecerreyes, D. *Small* **2006**, *2*, 507–512.

(65) Li, D.; Zhao, B. *Langmuir* **2007**, *23*, 2208–2217.

(66) Desset, S. L.; Cole-Hamilton, D. J. *Angew. Chem., Int. Ed.* **2009**, *48*, 1472–1474.

(67) Dorokhin, D.; Tomczak, N.; Han, M.; Reinhoudt, D. N.; Velders, A. H.; Vancso, G. J. *ACS Nano* **2009**, *3*, 661–667.

(68) Lee, J. C. M.; Bermudez, H.; Discher, B. M.; Sheehan, M. A.; Won, Y. Y.; Bates, F. S.; Discher, D. E. *Biotechnol. Bioeng.* **2001**, *73*, 135–145.

(69) Vriezema, D. M.; Garcia, P. M. L.; Oltra, N. S.; Natzakis, N. S.; Kuiper, S. M.; Nolte, R. J. M.; Rowan, A. E.; van Hest, J. C. M. *Angew. Chem., Int. Ed.* **2007**, *46*, 7378–7382.

(70) van Dongen, S. F. M.; Nallani, M.; Cornelissen, J. J. L. M.; Nolte, R. J. M.; van Hest, J. C. M. *Chem.—Eur. J.* **2009**, *15*, 1107–1114.

(71) The polymer was as previously synthesized via anionic polymerization: Davis, K. P.; Lodge, T. P.; Bates, F. S. *Macromolecules* **2008**, *41*, 8289–8291.

(72) Jain, S.; Bates, F. S. *Macromolecules* **2004**, *37*, 1511–1523.

(73) Simone, P. M.; Lodge, T. P. *Macromolecules* **2008**, *41*, 1753–1759.

(74) Won, Y. Y.; Davis, H. T.; Bates, F. S. *Macromolecules* **2003**, *36*, 953–955.

(75) Hayward, R. C.; Pochan, D. J. *Macromolecules* **2010**, *43*, 3577–3584.

(76) Meli, L.; Santiago, J. M.; Lodge, T. P. *Macromolecules* **2010**, *43*, 2018–2027.

(77) Hauschild, S.; Lipprandt, U.; Ruplecker, A.; Borchert, U.; Rank, A.; Schubert, R.; Forster, S. *Small* **2005**, *1*, 1177–1180.

(78) Lorenceau, E.; Utada, A. S.; Link, D. R.; Cristobal, G.; Joanicot, M.; Weitz, D. A. *Langmuir* **2005**, *21*, 9183–9186.

(79) Holowka, E. P.; Pochan, D. J.; Deming, T. J. *J. Am. Chem. Soc.* **2005**, *127*, 12423–12428.

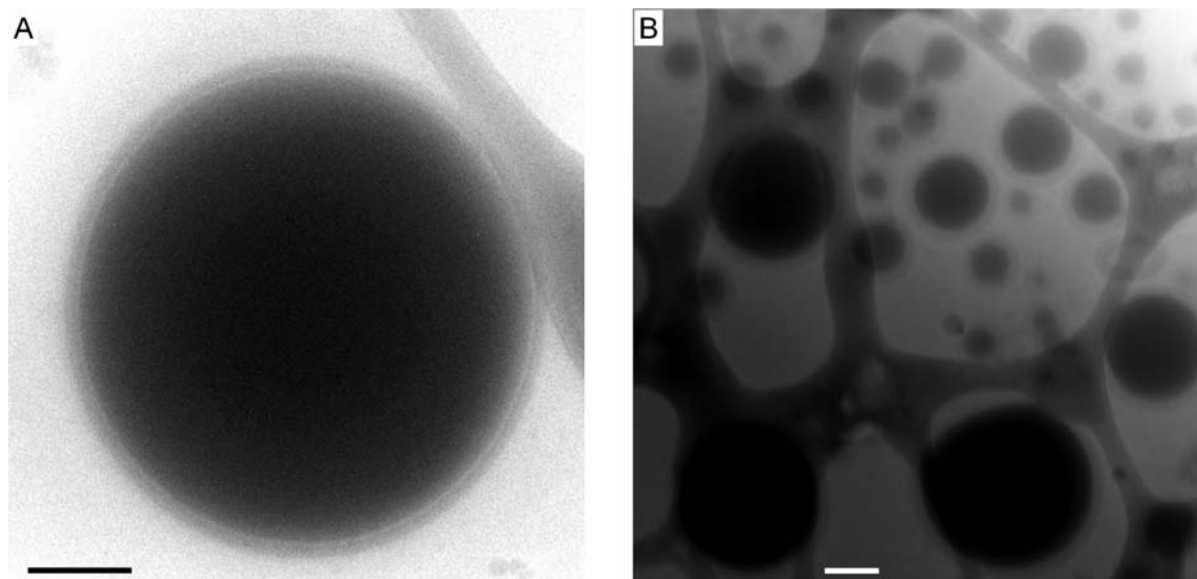


Figure 3. Cryo-TEM images of PB-PEO vesicles initially formed in [EMIM][TFSI] and then transferred to water with higher (A) and lower (B) magnification. Scale bars, 200 nm.

Vesicles with ionic liquid interiors dispersed in water were then prepared by spontaneous transfer of the PB-PEO block copolymer vesicles, initially formed in [EMIM][TFSI], to water through addition of water to the [EMIM][TFSI] solution of the vesicles at room temperature. Figure 3 shows representative cryo-TEM images of the vesicles after the transfer. The electron density difference between the aqueous matrix, PB membrane, and [EMIM][TFSI] interior, i.e., $\rho_{e,\text{aq.}} < \rho_{e,\text{PB}} < \rho_{e,[\text{EMIM}][\text{TFSI}]}$, enables direct visualization of the vesicle nanostructure in a light aqueous matrix, with a gray PB membrane and a dark [EMIM][TFSI] interior. It is evident from these images that the vesicles migrate intact during the transfer, so that their ionic liquid interiors are preserved. This is consistent with the intact transfer of the micelle shuttle previously reported^{49,62} and demonstrates the robustness of the PB membrane. It should be noted that the encapsulated ionic liquid in the vesicle interiors is protected against an osmosis-driven leakage to the external aqueous matrix, since the aqueous matrix is likely saturated rapidly by [EMIM][TFSI]⁸¹ prior to the vesicle transfer to water (which takes ca. 30 min with moderate agitation). The encapsulated ionic liquid is retained within the vesicle interior for at least 10 d after the transfer, as revealed by cryo-TEM (see Supporting Information). The stability of the vesicles is further demonstrated by dynamic light scattering analysis. The vesicles transferred into water have a mean hydrodynamic radius ($\langle R_h \rangle$) of 198 nm and a relatively broad size distribution indicated by a reduced second cumulant⁸² (μ_2/Γ^2) of 0.44. These values are essentially the same as those of the vesicles in [EMIM][TFSI] before the transfer ($\langle R_h \rangle = 193$ nm and $\mu_2/\Gamma^2 = 0.55$) and of the transferred vesicles in water 10 d after the transfer ($\langle R_h \rangle = 191$ nm and $\mu_2/\Gamma^2 = 0.42$). The retention of the vesicle structure during and after the transfer is also consistent with the stability

of PB-PEO micelles in both water^{72,74} and [EMIM][TFSI].⁷⁶ In summary, this simple protocol produces stable ionic liquid-in-water microemulsions, in which the ionic liquid pools are stabilized by a copolymer bilayer.

Detailed packing characteristics of the vesicles can be extracted from the cryo-TEM images. First, the membrane thickness (d) can be directly estimated from the cryo-TEM images. A d of 28 nm (± 2 nm) of the vesicles with [EMIM][TFSI] interiors dispersed in water is obtained, which is significantly larger than that of typical liposomes (3–4 nm).⁸³ The much thicker membrane of polymersomes has been recognized by Discher and co-workers as the source of the enhanced robustness of polymer vesicles,^{2,3} consistent with the stability of the vesicles observed here. The vesicles initially formed in both [EMIM][TFSI] and water have nearly the same d as the transferred vesicles in water, 28 and 29 nm, respectively; this is also consistent with the comparable solvent selectivity of water and [EMIM][TFSI] toward this diblock. Then, assuming that the PB membrane is free of other components (i.e., solvent and PEO), the interfacial area per chain (a_0) of the three kinds of vesicles can be simply calculated from the known d , the bulk density of PB,⁸⁴ and the molecular weight of the PB block. A relatively low a_0 of 0.9 nm² per chain is found, reflecting close packing of the chains⁸⁵ and a large aggregation number (p) (e.g., $p \approx 5 \times 10^5$ for a vesicle with a radius of 200 nm). In addition, the chain stretching factor (s) of the PB block can be estimated as $s \equiv d/(2\langle h_0^2 \rangle_{\text{PB}}^{1/2})$, where $\langle h_0^2 \rangle_{\text{PB}}^{1/2}$ is the root-mean-square end-to-end distance of unperturbed PB chain dimension;⁸⁶ a respectable $s \approx 1.5$ is obtained.

A particularly attractive feature of the vesicles with ionic liquid interiors dispersed in water is their facile recoverability. Similar to the transfer from [EMIM][TFSI] to water at room temperature, upon heating the vesicles in the aqueous phase

(80) Howse, J. R.; Jones, R. A. L.; Battaglia, G.; Ducker, R. E.; Leggett, G. J.; Ryan, A. J. *Nat. Mater.* **2009**, *8*, 507–511.

(81) The solubility of [EMIM][TFSI] in water is 0.046 mmol/g at room temperature: Freire, M. G.; Carvalho, P. J.; Gardas, R. L.; Marrucho, I. M.; Santos, L. M. N. B. F.; Coutinho, J. A. P. *J. Phys. Chem. B* **2008**, *112*, 1604–1610.

(82) A measure of the width of the micelle size distribution. See Supporting Information for a plot of the micelle size distribution: Koppel, D. E. *J. Chem. Phys.* **1972**, *57*, 4814–4820.

(83) Marsh, D. *CRC Handbook of Lipid Bilayers*; CRC Press: Boca Raton, FL, 1990.

(84) $\rho_{\text{PB}} = 0.87$ g/cm³. Fetters, L. J.; Lohse, D. J.; Richter, D.; Witten, T. A.; Zirkel, A. *Macromolecules* **1994**, *27*, 4639–4647.

(85) Battaglia, G.; Ryan, A. J. *J. Am. Chem. Soc.* **2005**, *127*, 8757–8764.

(86) $\langle h_0^2 \rangle_{\text{PB}}^{1/2} = 9.5$ nm, estimated using a statistical segment length of $b(\text{PB}) = 5.9$ Å. Hiemenz, P. C.; Lodge, T. P. *Polymer Chemistry*, 2nd ed.; CRC: New York, 2007.

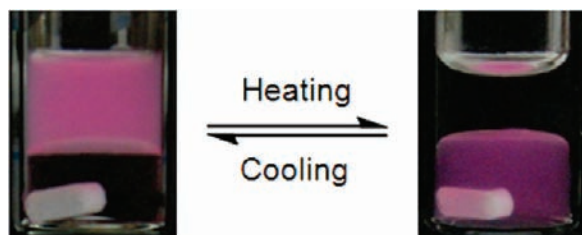


Figure 4. Images of the dye-loaded vesicle shuttle between water (upper phase) and [EMIM][TFSI] (lower phase). The vesicles were initially formed in [EMIM][TFSI] with Rho-PB loaded in the membrane, and the system was equilibrated at 22 (left) and 75 °C (right) and irradiated with daylight lamps.

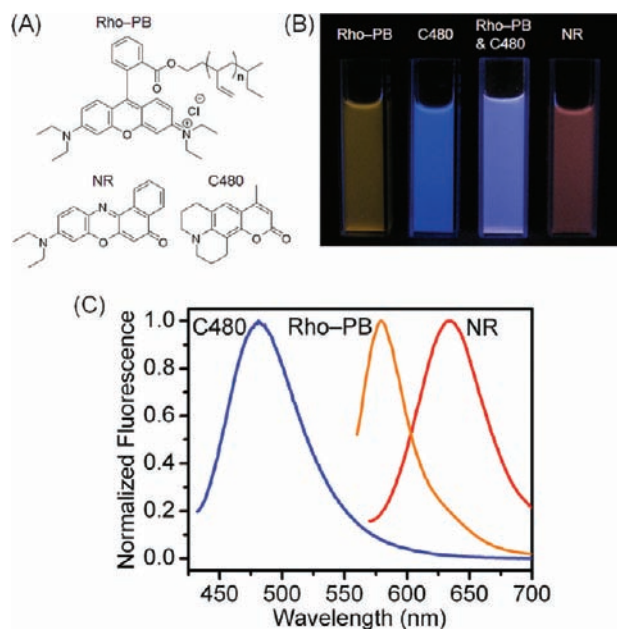


Figure 5. Molecular structures of Rho-PB, NR, and C480 (A), fluorescence images (B), and spectra (C) of the aqueous solutions of the dye-loaded vesicles with [EMIM][TFSI] interiors. The solutions were irradiated with a 254 nm UV lamp, and spectra were excited at 405 nm for C480 and 543 nm for Rho-PB and NR.

begin to migrate back to the ionic liquid phase at or above 60 °C (Figure 4). A reversible and quantitative partitioning of the vesicles in the biphasic system can be directly visualized from the cloudy appearance of the vesicle solution. The exclusive partitioning of the vesicles in the biphasic system into one phase or the other is consistent with previous thermodynamic studies on a spherical PB-PEO micelle shuttle (>99.5% partitioning) that revealed a very sensitive temperature dependence of the Gibbs free energy of partitioning.⁶² This sensitivity can be attributed to the large number of EO units in the vesicle corona, the preferred solvation of which ultimately drives the transfer.⁶²

In comparison with the spherical micelle shuttle, which can only transport solvophobic cargoes, the vesicle shuttle may transport both solvophobic cargoes in the vesicle membrane and cargoes soluble in the preparation phase (but perhaps not in the destination phase) in the vesicle interior. To demonstrate this, three fluorescent dyes were chosen as representative cargoes (Figure 5A). Rhodamine B conjugated with a PB homopolymer (2 kDa) (Rho-PB) is insoluble in both water and [EMIM][TFSI] but is fully soluble in the membrane.⁶² Nile Red (NR) and Coumarin 480 (C480) are both hydrophobic but soluble in [EMIM][TFSI] for interior loading. To assess whether NR or C480 may partition into the PB membrane of the vesicles to

any significant extent, a solution of 0.5 mM NR and 1 mM C480 in a biphasic system containing equal volumes of [EMIM][TFSI] and a PB homopolymer (2 kDa) was analyzed using UV-vis spectroscopy. Both dyes have an overwhelming preference for [EMIM][TFSI] over PB, i.e., with [EMIM][TFSI]/PB partition coefficients larger than 100, which is not surprising considering their polarity,⁸⁷ and confirms a selective loading of the two dyes into the vesicle interior.

The dyes are initially loaded in the vesicle membrane or encapsulated in the vesicle interior in [EMIM][TFSI] and then transported to water via the vesicle migration. Figure 5B shows fluorescence images of the aqueous solutions of the transferred dye-loaded vesicles, featuring the distinct orange, red, and blue emission of the loaded Rho-PB, NR, and C480, respectively. The solutions were further characterized by fluorescence spectroscopy (Figure 5C). In particular, NR is a widely used solvatochromic dye, showing sensitive response to solvents with varying polarity,⁸⁸ which can thus be used to probe the microenvironment of the vesicles. The fluorescence peak of the aqueous NR-loaded vesicle solution, located at 636 nm, indicates that the polarity of the enclosed ionic liquid pool is similar to short chain alcohols, which is consistent with previous polarity studies on ionic liquids.^{87,89} Again, the reverse transport of the dyes by the vesicles back to [EMIM][TFSI] is straightforward upon heating. The loading of the fluorescence dyes also facilitates imaging of the vesicles using LSCM, which, as a complement to cryo-TEM, can identify the locus of dye loading, provide three-dimensional structural information, and easily capture vesicles with larger size, i.e., on the micrometer scale. For example, Figure 6A shows a representative two-dimensional LSCM image of Rho-PB-loaded vesicles in [EMIM][TFSI]. The orange rings confirm that the solvophobic Rho-PB is selectively loaded in the vesicle membrane.⁹⁰ Likewise, the encapsulation of NR and C480 in the [EMIM][TFSI] interiors of the vesicles in water is revealed by the filled red and blue circles, respectively, in Figure 6B and 6C. The spatial structure of the dye-loaded vesicles with [EMIM][TFSI] interiors in water is then characterized by scanning in the third dimension (Z). Figure 6D and 6E displays series of images of a single vesicle with membrane and interior loading, respectively, with 0.5 μm steps in the Z direction, thereby offering a view on the full encapsulation of the ionic liquid pool by the membrane in water.

Simultaneous loading and transport of cargoes in the vesicle membrane and interior were also achieved. Figure 5B displays the fluorescence image of an aqueous solution of vesicles with Rho-PB and C480 selectively and simultaneously loaded in their membrane and [EMIM][TFSI] interior, respectively. As the emission peaks of Rho-PB and C480 are well separated (Figure 5C), the two dyes can be separately imaged by LSCM using suitable excitation and detection channels, as shown by the selective imaging of Rho-PB in the membrane in Figure 7A and of C480 in the [EMIM][TFSI] interior in Figure 7B. These two images are then overlaid to generate an image of the vesicles with orange membranes and blue [EMIM][TFSI] interiors in Figure 7C. A further illustration of the dye loading is shown

(87) Reichardt, C. *Green Chem.* **2005**, *7*, 339–351.

(88) Fletcher, K. A.; Storey, I. A.; Hendricks, A. E.; Pandey, S.; Pandey, S. *Green Chem.* **2001**, *3*, 210–215.

(89) Carmichael, A. J.; Seddon, K. R. *J. Phys. Org. Chem.* **2000**, *13*, 591–595.

(90) It should be noted that the vesicle membrane appears significantly larger than that observed by cryo-TEM, as LSCM has lower resolution than cryo-TEM, i.e., a depth field of about 400 nm in the current setup.

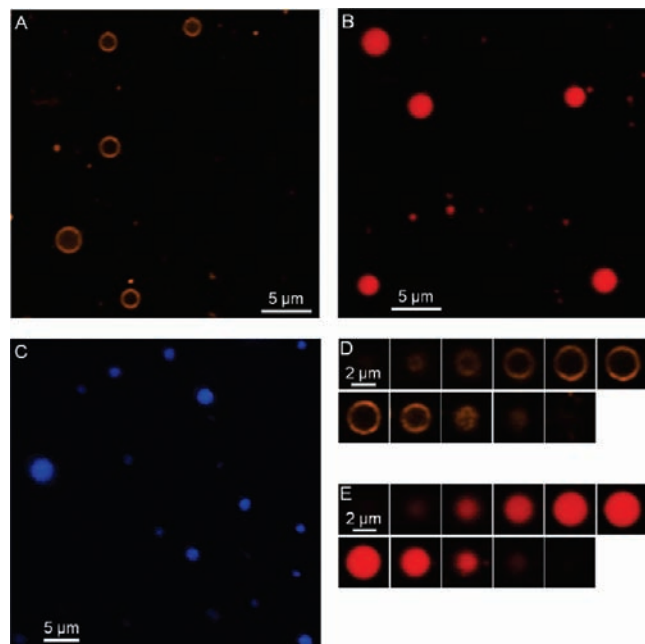


Figure 6. LSCM images of vesicles in [EMIM][TFSI] loaded with water and [EMIM][TFSI]-insoluble Rho-PB in the membrane (A) and vesicles with [EMIM][TFSI] interiors dispersed in water that are loaded with hydrophobic but [EMIM][TFSI]-soluble NR (B) and C480 (C) in the interior, and Z-scan LSCM images of a single vesicle with [EMIM][TFSI] interior dispersed in water that is loaded with Rho-PB on the membrane (D) and NR in the interior (E), where *XY* cross sections were taken in 0.5 μm steps in *Z* from the bottom (upper left) up.

by the fluorescence intensity profile of a double dye-loaded vesicle in Figure 7D.

Conclusions

We demonstrated polymersomes with hydrophobic ionic liquid interiors dispersed in water. The vesicles are readily prepared by a spontaneous transfer of PB-PEO block copolymer vesicles from [EMIM][TFSI] to water, where interestingly and importantly the two solvents are immiscible yet have similar selectivity for PB-PEO block copolymers. A relatively high molecular weight PB-PEO block copolymer is used to produce stable and robust vesicles that are able to migrate with their ionic liquid interiors intact across the water/[EMIM][TFSI] interface, leading to bilayer-stabilized ionic liquid-in-water microemulsions. Further stabilization of the vesicle structure is feasible by cross-linking the PB membrane.⁹¹ Cryo-TEM analysis of the vesicles confirms the nanostructure and provides detailed packing characterization. Quantitative recovery of the vesicles is straightforward by reverse transfer back to [EMIM][TFSI] upon heating.

The transport capability of the shuttling system is demonstrated by reversible delivery of distinct hydrophobic dyes from [EMIM][TFSI] to water, selectively and simultaneously in the vesicle membrane and interior. The loaded fluorescence dyes enable the probing of the microenvironment of the vesicular ionic liquid interior through solvatochromism and characteriza-

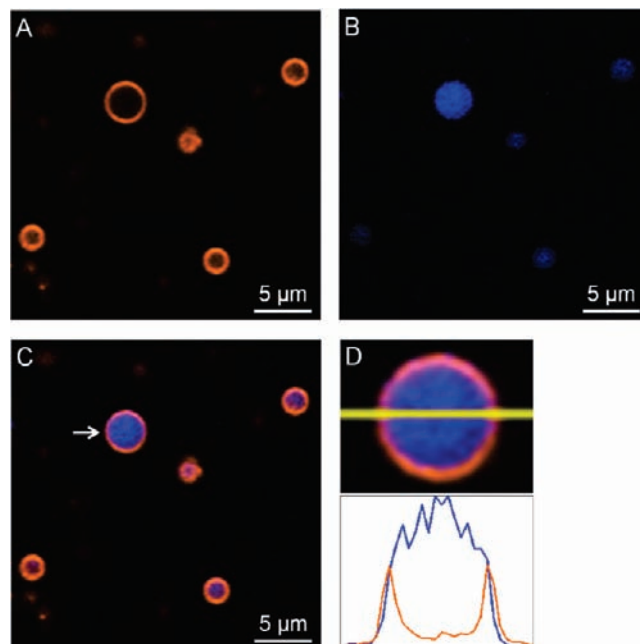


Figure 7. LSCM images of vesicles with [EMIM][TFSI] interiors in water that are simultaneously and selectively loaded with Rho-PB on the membrane and C480 in the interior: selective imaging of vesicle membrane (A) using a laser with a wavelength of 543 nm and a detection channel with a range of 560–660 nm and vesicle interior (B) using a laser with a wavelength of 405 nm and a detection channel with a range of 480–490 nm, and their overlay (C), and fluorescence intensity profile (D) of the Rho-PB- and C480-loaded vesicle indicated by the white arrow in C along the yellow line.

tion of the vesicles by LSCM. This system is of particular interest as nanocarriers or nanoreactors for reactions, catalysis, and separations involving ionic liquids. Permeability across the polymer membrane is important for many of these applications. The liquid PB membrane, i.e., the glass transition temperature $T_{g,\text{PB,bulk}} = -12\text{ }^\circ\text{C}$,⁹² may suggest favorable permeation,^{2,93} which is currently under investigation.

Acknowledgment. This work was supported by the National Science Foundation through Award DMR-0804197 and by the Frieda Martha Kunze Fellowship (Z.B.). Parts of this work were carried out in the Characterization Facility, University of Minnesota, which receives partial support from the NSF through the MRSEC program. We acknowledge Dr. Kevin P. Davis for generous supply of the block copolymer, Prof. Valerie C. Pierre for providing access to the UV-vis and fluorescence spectrophotometers, and Dr. Chun Liu and Dr. Kevin P. Davis for help in the initial cryo-TEM experiments.

Supporting Information Available: Experimental details, DLS results, cryo-TEM images, and complete ref 9. This material is available free of charge via the Internet at <http://pubs.acs.org>.

JA107751K

(91) Discher, B. M.; Bermudez, H.; Hammer, D. A.; Discher, D. E.; Won, Y. Y.; Bates, F. S. *J. Phys. Chem. B* **2002**, *106*, 2848–2854.

(92) Ferry, J. D. *Viscoelastic Properties of Polymers*, 3rd ed.; Wiley: New York, 1980.

(93) Leson, A.; Filiz, V.; Forster, S.; Mayer, C. *Chem. Phys. Lett.* **2007**, *444*, 268–272.